

Supplement of Atmos. Chem. Phys., 20, 13655–13670, 2020  
<https://doi.org/10.5194/acp-20-13655-2020-supplement>  
© Author(s) 2020. This work is distributed under  
the Creative Commons Attribution 4.0 License.



Atmospheric  
Chemistry  
and Physics  
Open Access  
EGU

*Supplement of*

## **Investigation of the wet removal rate of black carbon in East Asia: validation of a below- and in-cloud wet removal scheme in FLEXible PARTICle (FLEXPART) model v10.4**

**Yongjoo Choi et al.**

*Correspondence to:* Yongjoo Choi ([choingjoo@jamstec.go.jp](mailto:choingjoo@jamstec.go.jp))

The copyright of individual parts of the supplement might differ from the CC BY 4.0 License.

## S1 Uncertainty in the transport efficiency (TE) and below- and in-cloud scavenging coefficients

Our main results, including the TE,  $\Lambda_{\text{below}}$ , and  $\Lambda_{\text{in}}$ , could be influenced by selecting (1) different starting altitudes of the backward trajectories and (2) different altitude criteria for identifying the potential emission region.

First, to investigate the uncertainty caused by different starting altitudes of the backward trajectories, we analyzed the Welch's *t*-test for APT derived from starting altitudes of 500 m and 1000 m. The APT between the two datasets did not show a significant difference (3%) ( $p \geq 0.1$ ). Depending on the site, the TE showed a significant difference ( $p < 0.05$ ) at Gosan only at a relatively small value of  $-4.2\%$ . In the case of regional TE, Northeast China and South Korea were significantly different ( $p < 0.01$ ), with original values up to  $-15\%$ ; however, the corresponding APT for achieving TE=0.5 and TE=1/*e* only decreased by  $-6\%$  and  $-2\%$ , respectively. The regional wet removal efficiency was more apparent, such as more or less APT needed to attain TE=0.5 and TE=1/*e* in low-efficiency regions (East and North China) and high-efficiency regions (South Korea and Japan), respectively. For the high starting altitude, i.e., 1000 m, the air mass had a higher chance of being exposed to in-cloud scavenging resulting in a much lower TE for in-cloud scavenging ( $-3\%$ ). Otherwise, the TE for below-cloud scavenging cases was increased by 7% because of a reduced chance to expose washout effects (Table S1). Because of the variations in the TE for below- and in-cloud scavenging cases, the calculated median  $\Lambda_{\text{below}}$  and  $\Lambda_{\text{in}}$  converged within a similar range as the original results. It should be noted that the median measured  $\Lambda_{\text{below}}$  was slightly higher than the calculated  $\Lambda_{\text{below}}$  according to FLEXPART, which is opposite the original results. The small difference could be ignored when considering the insufficient sample number for below-cloud cases at a starting altitude of 1000 m.

Second, we also checked the difference in wet scavenging efficiency, which can be caused by applying 1.5 km (instead of 2.5 km) as a threshold to determine the potential emission region. The identified six administrative districts for potential emission regions at an altitude of 1.5 km were same as those at an altitude of 2.5 km. The median traveling time from potential source regions to receptor sites was decreased from 38 h to 25 h when precipitation occurred because the individual potential source region was closer to the receptor site because the selection altitude was decreased. However, the difference in traveling time did not significantly influence our final results because the TE for below- and in-cloud cases only decreased by 1% and 6% and the measured  $\Lambda_{\text{below}}$  and  $\Lambda_{\text{in}}$  were consistent with the original results within  $\pm 54\%$  (Table S2). From these results, we confirmed the representativeness of our regional and seasonal wet removal efficiency analysis.

## S2 Difference in air mass pathways and accumulated precipitation along trajectory (APT) between HYSPLIT and FLEXPART

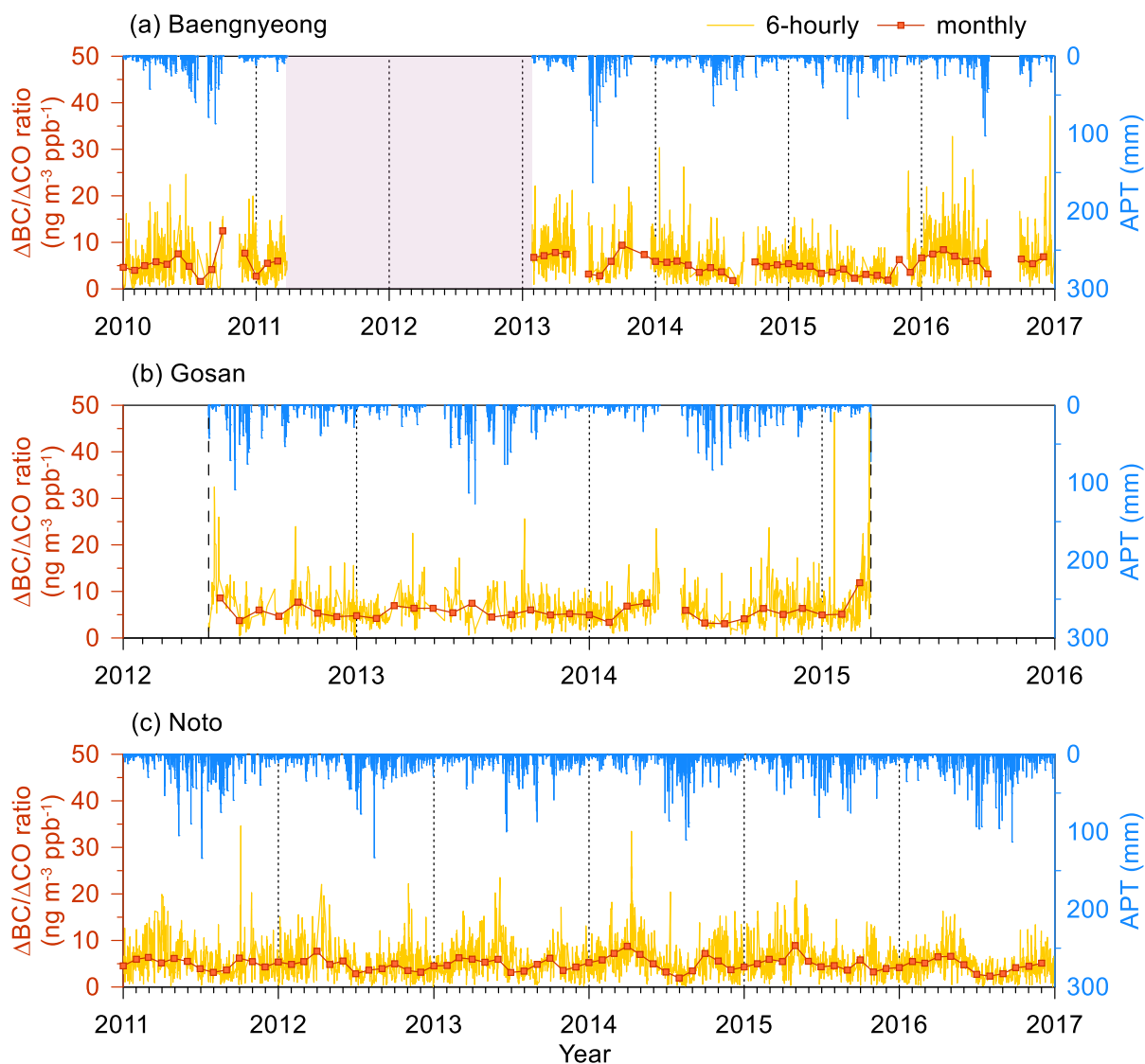
We investigated the uncertainty in the air mass pathway and APT between HYSPLIT model using ERA5 and FLEXPART using ERA-Interim during study periods at three sites. It should be noted that the trajectory of FLEXPART was selected as the center of the main grid ( $1^\circ \times 1^\circ$ ) according to the highest residence time in the same time interval and then compared with HYSPLIT results by calculating the distance between two hourly endpoints. Thus, differences of less than  $\sim 100$  km can be regarded as a good agreement when considering the grid resolution of FLEXPART. The difference in distance increased as the traveling time was increased. However, the median traveling time of air masses, including APT=0 case, was 31 h, which showed a difference in distance of  $\sim 100$  km. When the traveling time was expanded up to the 75%ile of the traveling time (50 h), the difference in distance was close to  $\sim 200$  km. Although the difference in distance at 72 h traveling time was high, 72 h traveling time cases was so rare that we could neglect the impacts on our results. In total, the median difference in distance was  $\sim 47$  km, suggesting good agreement between the two datasets. In addition, the difference in accumulated backward-trajectory endpoints was much smaller because random errors in the single calculations can be diminished by increasing the number of calculations (Gebhart et al., 2005; Jeong et al., 2017).

Figure S2 presents the cumulative probability of APT from HYSPLIT and FLEXPART. Although the air mass pathway showed insignificant differences between the two models, the median APT of FLEXPART (1.2 mm) was two times higher than that of HYSPLIT (0.63 mm), indicating a higher bias of the FLEXPART APT. This result can be caused by the difference in meteorological input data and the treatment of precipitation fields, homogeneous precipitation in a single grid cell ( $0.25^{\circ} \times 0.25^{\circ}$ ) in HYSPLIT and disaggregated precipitation induced by interpolating in time and space in FLEXPART (Hittmeir et al., 2018). The higher bias in the FLEXPART APT contributed to increasing the magnitude of the underestimation of FLEXPART TE when assuming the same APT from HYSPLIT model, indicating an insignificant impact on the results.

Gebhart, K.A., Schichtel, B.A., Barna, M.G.: Directional biases in back trajectories caused by model and input data. *J. Air Waste Manag.* 55, 1649-1662, 2005.

Jeong, U., Kim, J., Lee, H., Lee, Y.G.: Assessing the effect of long-range pollutant transportation on air quality in Seoul using the conditional potential source contribution function method. *Atmos. Environ.*, 150, 33-44, 2017.

Hittmeir, S., Philipp, A., and Seibert, P.: A conservative reconstruction scheme for the interpolation of extensive quantities in the Lagrangian particle dispersion model FLEXPART. *Geosci. Model Dev.*, 11, 2503-2523, <https://doi.org/10.5194/gmd-11-2503-2018>, 2018.



**Figure S1.** Time series of the  $\Delta BC/\Delta CO$  ratio and accumulated precipitation along trajectory (APT) during the measurement periods in (a) Baengnyeong (1 Jan 2010–31 Dec 2016), (b) Gosan (1 May 2012–30 Apr 2015), and (c) Noto (1 Jan 2011–31 Dec 2016). The square symbols with solid lines indicate monthly concentrations. The red shaded region in the Baengnyeong figure indicates periods of data missing from 2011 to 2012 due to the absence of CO data.

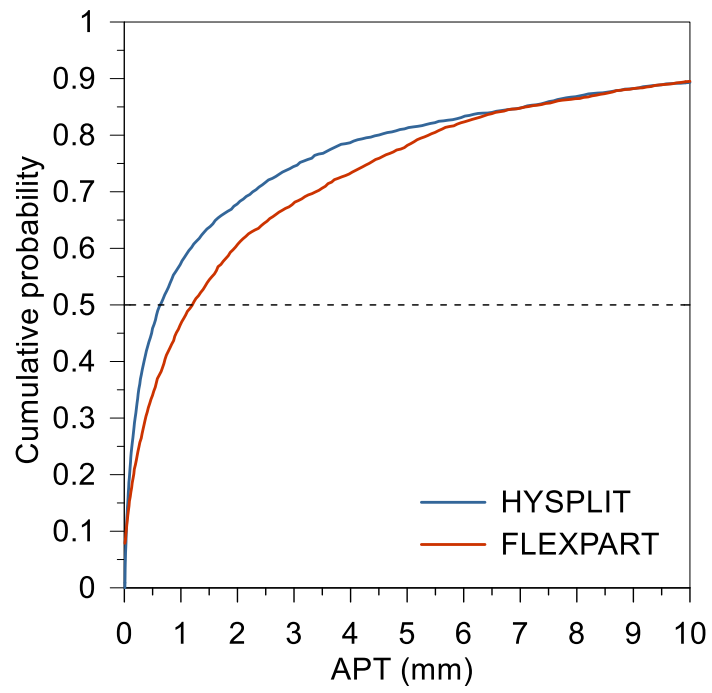


**Figure S2.** Cumulative probability plot of the APT from HYSPLIT (blue) and FLEXPART (red) during the study periods at the three sites. The dashed black line indicated a cumulative probability at 0.5 (median).

**Table S1.** Same as Table 2 except for the different backward trajectory starting altitudes (1000 m)

Cases	Median	Interquartile range (25 <sup>th</sup> percentile – 75 <sup>th</sup> percentile)
(a) Below cloud ( $N_{case} = 262$ )		
TE	0.95	[0.65 – 1.28]
Measured $\Lambda_{below}$ ( $s^{-1}$ )	$8.85 \times 10^{-6}$	$[6.57 \times 10^{-6} - 1.46 \times 10^{-5}]$
Calculated $\Lambda_{below}$ ( $s^{-1}$ ) <sup>a</sup>	$7.49 \times 10^{-6}$	$[6.83 \times 10^{-6} - 8.42 \times 10^{-6}]$
(b) In-cloud ( $N_{case} = 953$ )		
TE	0.70	[0.46 – 1.02]
Measured $\Lambda_{in}^*$ ( $s^{-1}$ ) <sup>b</sup>	$7.67 \times 10^{-5}$	-
Calculated $\Lambda_{in}^*$ ( $s^{-1}$ ) <sup>a,b</sup>	$8.01 \times 10^{-6}$	-

<sup>a)</sup> Calculated using FLEXPART scheme

<sup>b)</sup> Overall median value

**Table S2.** Same as Table 2 except for the different altitude criteria (1.5 km) for identifying potential emission source regions.

Cases	Median	Interquartile range (25 <sup>th</sup> percentile – 75 <sup>th</sup> percentile)
(a) Below cloud ( $N_{case} = 436$ )		
TE	0.88	[0.60 – 1.24]
Measured $\Lambda_{below}$ ( $s^{-1}$ )	$6.17 \times 10^{-6}$	$[2.55 \times 10^{-6} - 1.39 \times 10^{-5}]$
Calculated $\Lambda_{below}$ ( $s^{-1}$ ) <sup>a</sup>	$7.52 \times 10^{-6}$	$[6.88 \times 10^{-6} - 8.50 \times 10^{-6}]$
(b) In-cloud ( $N_{case} = 282$ )		
TE	0.68	[0.44 – 1.03]
Measured $\Lambda_{in}^*$ ( $s^{-1}$ ) <sup>b</sup>	$9.39 \times 10^{-5}$	-
Calculated $\Lambda_{in}^*$ ( $s^{-1}$ ) <sup>a,b</sup>	$8.15 \times 10^{-6}$	-

<sup>a)</sup> Calculated using FLEXPART scheme

<sup>b)</sup> Overall median value